IL NUOVO CIMENTO Vol. 35 C, N. 1 Gennaio-Febbraio 2012
DOI 10.1393/ncc/i2012-11125-9

Colloquia: LaThuile11

Cosmic rays in the TeV region with the ARGO-YBJ detector

P. Bernardini for the ARGO-YBJ Collaboration
Dipartimento di Fisica, Università del Salento and INFN, Sezione di Lecce - Lecce, Italy

(ricevuto il 29 Settembre 2011; pubblicato online il 23 Gennaio 2012)

Summary. — Very High Energy (VHE) γ-astronomy and cosmic ray physics are the main goals of the ARGO-YBJ experiment. The detector is located in Tibet (People's Republic of China) and is a full-coverage Extensive Air Shower array consisting of a carpet of Resistive Plate Chambers (RPCs). Altitude and full coverage ensure an unprecedented reconstruction of showers close to their maximum size. The performances of the detector and the present results concerning TeV cosmic ray physics will be presented.

PACS 96.50.sd – Extensive air showers.

1. – Introduction

The ARGO-YBJ (Astrophysical Radiation Ground-based Observatory at YangBaJing) experiment is located in Tibet at an altitude of 4300 m and is supported by an Italian-Chinese scientific collaboration. It is mainly devoted to VHE gamma astronomy and cosmic ray (CR) physics.

After some detail about the performances of the detector (sect. **2**), this paper will be focused on CRs in the range 1–300 TeV. Many significant analyses have been completed or are under way about Moon shadow and antiproton flux (sect. **3**), anisotropies (sect. **4**) and proton cross section (sect. **5**). Unprecented details on the shower front are available (sect. **6**) thanks to the high granularity and this information can be crucial to test the hadron interaction models. Other CR topics (as the spectrum measurement, the large-scale anisotropy or the Sun shadow analysis) will not be discussed for space limits.

2. – Detector features and performance

The detector consists of a single layer of RPCs operated in streamer mode [1], on a total area of about $110 \times 100\,\mathrm{m}^2$ (fig. 1). The central carpet ($78 \times 74\,\mathrm{m}^2$) is fully active and surrounded by a sampling ring with other $1000\,\mathrm{m}^2$ (20% of the outer ring) equipped with RPCs. The detector is logically divided in 153 clusters, each made by 12 RPCs with a dedicated Local Station for the DAQ. The digital read-out of the RPCs is performed by means of inductive strips ($6 \times 62\,\mathrm{cm}^2$) well suited to detect small air showers. The

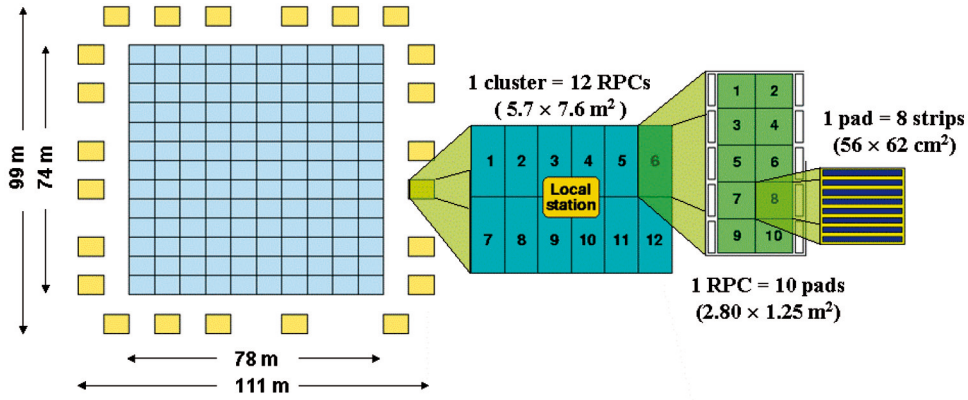

Fig. 1. – (Colour on-line) Setup of the ARGO-YBJ experiment. Two big-pads (not shown in this figure) are used for the analog charge read-out of each RPC.

fast-OR of 8 strips is called *pad* and defines the space-time pixel of the detector, with a time resolution of ~ 1.8 ns [2]. The timing calibration of the detector has been properly performed by means of an innovatory software method [3] and does not require dedicated calibration runs. Thus the data-taking is limited only by mantainance operations and the duty-cycle is higher than 86%. In order to extend the measurable energy range, each RPC has been equipped also with two large electrodes, called *big pads*, which provide an analog signal proportional to the deposited charge [4].

ARGO-YBJ collects data in scaler and shower mode. The first one does not require any trigger, it records the rate for four multiplicity bands (≥ 1, ≥ 2, ≥ 3 and ≥ 4) on each cluster in a time window of 0.5 s. The scaler mode allows the detection of low energy transient phenomena (*e.g.*, GRBs and solar flares) observed as non-statistical fluctuations of the background [5].

The shower mode works when the number of pads fired in a time-window of 420 ns exceeds the multiplicity required by the trigger condition. Typically the lowest multiplicity is 20 and the trigger rate is 3.5 kHz. The event is fully reconstructed (arrival direction, core position, lateral distribution and so on) looking at the space-time pattern (see fig. 2) and the size of the shower is measured by means of the fired strips. When the strip signal is saturated as in the event of fig. 3, a detailed reconstruction of the shower is always allowed by the recently implemented charge read-out. Because of this detector capability the CR studies can be extended to some thousands of TeV, in the region close to the knee.

Thanks to modularity the data-taking began during the commissioning, the central carpet was completed in 2006. Since November 2007 the experiment has been fully installed and in stable data-taking.

3. – Moon shadow and antiproton flux

Cosmic rays are hampered by the Moon, therefore a deficit of CRs in its direction is expected (the so-called Moon shadow). The same effect has been observed in the direction of the Sun [6]. The Moon shadow analysis is a crucial test of the detector

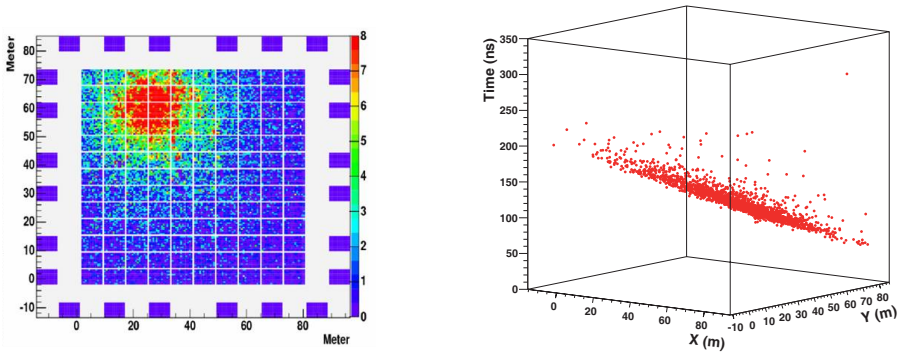

Fig. 2. – (Colour on-line) Digital display of ARGO-YBJ events. Left: x-y shower footprint, where the color scale indicates the number of strips fired on each pad. Right: x-y-time view of another shower, where each dot is a fired pad.

performance. The RMS of the deficit is related to the Point Spread Function (PSF) of the detector according to

$$RMS = \sqrt{\sigma^2 + \left(\frac{\phi}{4}\right)^2}, \tag{1}$$

where σ^2 is the variance of a Gaussian PSF and $\phi = 0.52^\circ$ is the Moon angular diameter. The westward angular shift $\Delta\alpha$ of the shadow is due to the bending of CR path in the geomagnetic field and allows to calibrate the scale of the primary energy (E) according to the formula $\Delta\alpha \sim 1.58^\circ Z/E[\mathrm{TeV}]$. Finally the deficit position for events with high rigidity (that is energy) allows to estimate the pointing accuracy.

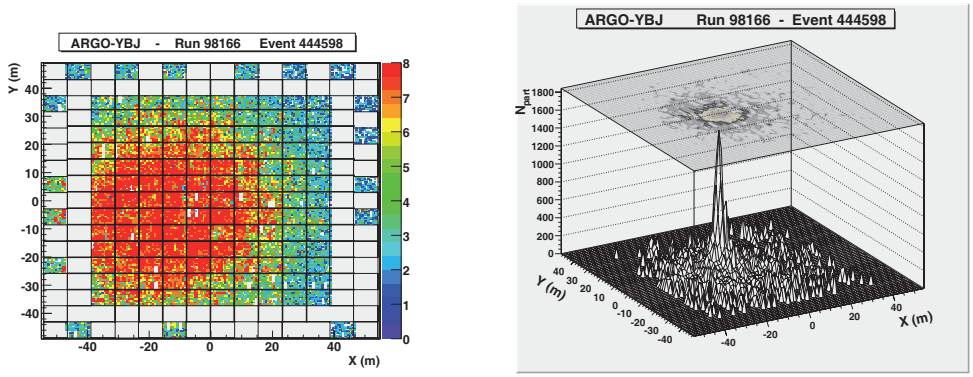

Fig. 3. – (Colour on-line) Comparison between digital and analog read-out for a high-energy event. Left: the large number of particles saturates the digital response (8 strips fired for each pad). Right: the shower core is clearly visible in the analog reconstruction (the number of particles is on the vertical axis).

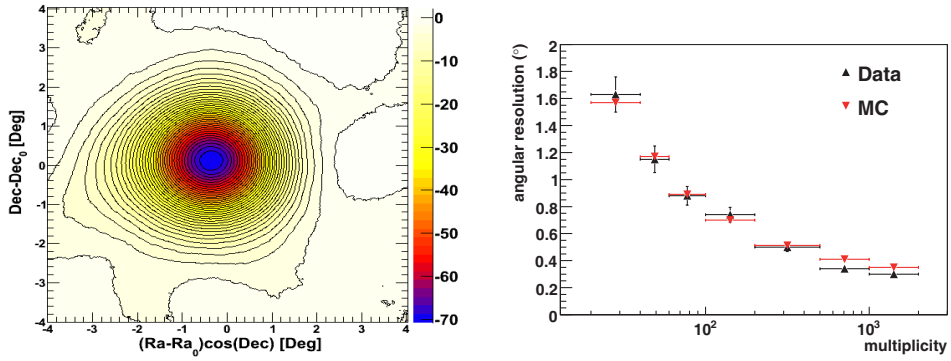

Fig. 4. – (Colour on-line) Moon shadow. Left: significance map of the Moon region. The color scale gives the deficit standard deviations. Right: angular resolution as a function of strip multiplicity. Real data and MC simulation are compared.

The data analysis (fig. 4) confirms the reliability of the ARGO-YBJ detector. The Moon shadow is observed with a significance of 9 standard deviations (s.d.) per month at TeV energy. Using the data collected in the period July 2006–November 2010 and requiring more than 100 strips fired in each event, the deficit appears with a significance higher than 70 s.d. (fig. 4, left). The Moon position turned out to be stable at a level of 0.1°. The angular resolution (fig. 4, right) is what expected.

Also the analysis of the primary CR bending due to the Earth magnetic field and the comparison with MC simulation [7] make us confident in the detector performaces and in the reconstruction algorithms. In fig. 5, left the westward Moon shadow shift is shown as a function of strip multiplicity or rigidity assuming positive charged primary CRs. On the contrary it is meaningful to take into account that primary antiprotons are deflected in the opposite sense in their way to the Earth. Thus the Earth-Moon system acts as a magnetic spectrometer and allows the search for antiparticles in the opposite direction of the observed Moon shadow. Selecting CRs with low enough energy and exploiting the

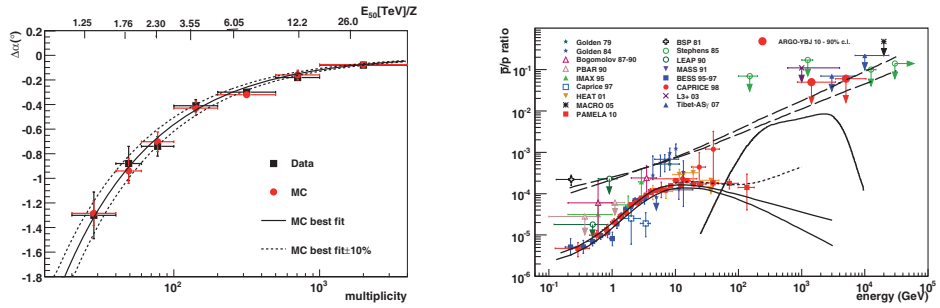

Fig. 5. – (Colour on-line) Left: westward shift ($\Delta\alpha$) of the Moon shadow as a function of strip multiplicity. Real data (black squares) and Monte Carlo simulation (red circles) are compared. The upper scale refers to the rigidity associated to the median energy in the multiplicity bins. Right: antiproton/proton ratio in the CR flux *vs.* energy. The upper limits set by ARGO-YBJ (red arrows) are compared with all measurements and with some theoretical estimate (see text).

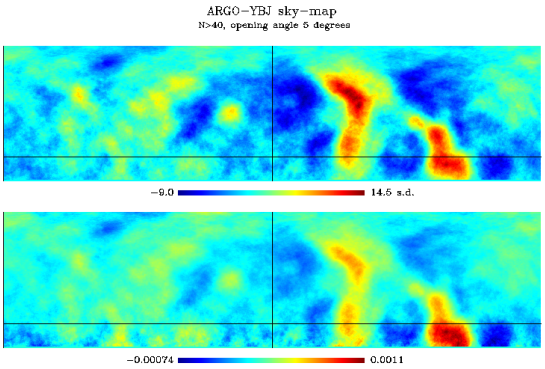

Fig. 6. – (Colour on-line) Sky-map in celestial coordinates of 3-years ARGO-YBJ data (opening angle 5°). Upper plot: the color scale indicates the statistical significance in s.d. Lower plot: the color scale indicates the percentage excess with respect to the estimated background.

angular resolution of the detector two shadows could be observed, one shifted towards West due to the positive CRs and the other one shifted towards East due to antiprotons.

The search for an antiproton signal has been performed exploiting the angular resolution, the pointing accuracy, the long-term stability and the low energy threshold of the detector [8]. The results are two upper limits shown in fig. 5, right, where also theoretical models are shown. The solid curves refer to $\bar{p}$ production during the CR propagation in the Galaxy [9], the long-dashed lines refer to primary antiproton production by antistars [10]. The dot-dashed line represents the contribution of $\bar{p}$ from the annihilation of heavy dark matter particles [11]. The short-dashed line shows a model [12] with secondary antiprotons and an additional antiproton component produced and accelerated at CR sources.

4. – Intermediate-scale anisotropies

The data collected in three years by the ARGO-YBJ detector show several few-degree CR excesses (fig. 6) after the removal of large angular features. This observation has high statistical significance and confirms findings by other experiments like Tibet AS-γ and Milagro. The morphological description of the phenomenon has been improved by our measurement and new localized sky zones hosting excesses have been found. Energy spectra have been measured and they are rather similar to previous measurements, though significant differences can be appreciated. So far these few-degrees anisotropies in the rigidity region 1–10 TV are not explained in terms of the standard theories of CR propagation in the galaxy. Possible explanations are a particular structure of the galactic magnetic field in the Earth neighborhood as well as the emission from nearby sources. In the last case few-degree anisotropies may reveal as an effective tool to probe the accelerated emission of CRs at sources.

5. – Proton cross section

The measurement [13] is based on the shower flux attenuation for different zenith angles (θ), *i.e.* atmospheric depths. The detector features allow to fix the energy ranges and

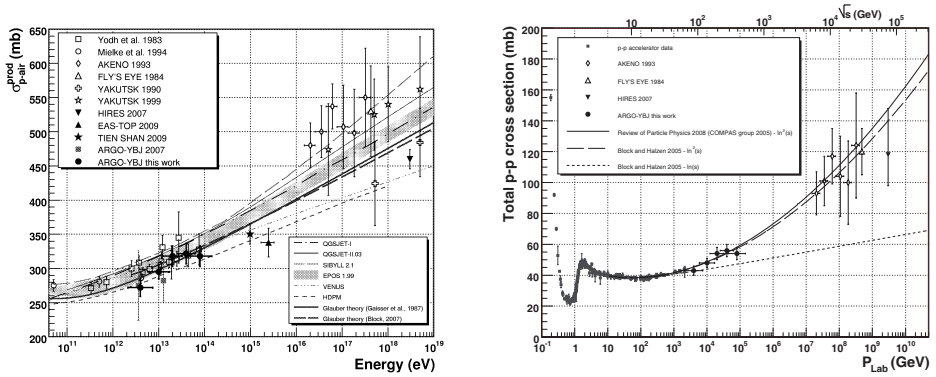

Fig. 7. – Left: the proton-air *production* cross section as measured by ARGO-YBJ and by other CR experiments. The predictions of several hadronic interaction models are also shown. Right: the p-p total cross section obtained by ARGO-YBJ data, together with results published by other CR and accelerator experiments.

to constrain the shower ages. In particular, different strip multiplicity intervals have been used to select showers corresponding to different primary energies. At the same time the information on particle density, lateral profile and shower front extension have been used to select showers having their maximum development within a given distance/grammage from the detection level. This made possible the unbiased observation of the expected exponential falling of shower intensities as a function of the atmospheric depth through the sec θ distribution. After the event selection, the fit to this distribution with an exponential law gives the slope value γ, connected to the characteristic length Λ through the relation $\gamma = h_0/\Lambda$ ($h_0 \simeq 610\,\mathrm{g/cm^2}$ is the vertical atmospheric depth). That is,

$$I(\theta) = A(\theta)\ I(0)\ e^{-\gamma\ (\sec\ \theta - 1)}, \tag{2}$$

where $A(\theta)$ accounts for the geometrical acceptance in the angular bin. The parameter Λ is connected to the proton interaction length by the relation $\Lambda = k\lambda_{int}$, where k depends on hadronic interactions and on the shower development in the atmosphere and its fluctuations. The actual value of k has been evaluated by a full MC simulation and it depends also on the experimental approach, the primary energy range and on the detector response. The p-air *production* cross section is then obtained from the relation

$$\sigma_{p\text{-}air}\ (\mathrm{mb}) = 2.41 \times 10^4/\lambda_{int}\ (\mathrm{g/cm^2}), \tag{3}$$

while several theoretical approaches are possible to get the corresponding p-p total cross section $\sigma_{p\text{-}p}$ [14]. The results of this measurement are shown in fig. 7 for 5 energies. ARGO-YBJ experimental points lie in an energy region not yet reached by p-p colliders (and still unexplored by p-$\bar{\mathrm{p}}$ experiments), favouring the asymptotic $\ln^2(s)$ increase of total hadronic cross sections.

6. – Morphology of the shower front

The space-time structure of extensive air showers depends on primary mass, energy and arrival direction and on the interaction mechanisms with air nuclei. Detailed

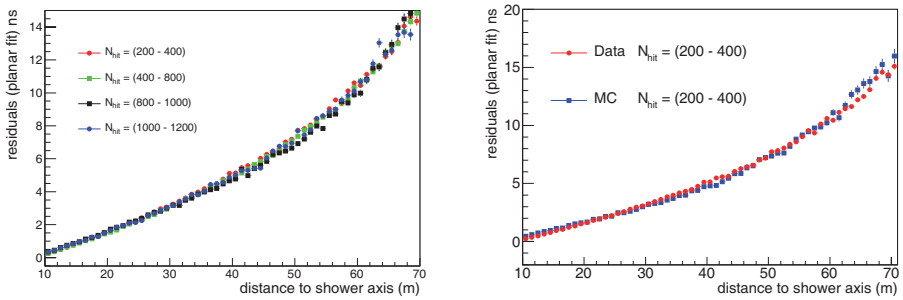

Fig. 8. – (Colour on-line) Mean of time residuals with respect to a planar fit as a function of the distance to shower axis. Left: real data measurement for different pad multiplicities. Right: real data and simulated data (proton) for pad multiplicity in the range 200–400.

measurements of many shower parameters (size, lateral distribution, arrival times, curvature and so on) would be required for a complete knowledge of the shower event.

A full-coverage array like ARGO-YBJ measures the arrival times and densities of shower particle at ground. The digital readout allows detection down to very low density and the high space-time granularity provides a fine sampling of the shower front close to the core. These unprecedented detector features allow deep studies about the shower development searching for more information about type of primary, its energy and shower age. These studies could be also a test-bed for hadronic interaction models and could give some hint about gamma-hadron separation.

The curvature and the thickness of the shower disc have been studied as a function of the distance to shower axis up to a maximum distance of 70 m for quasi-vertical showers ($\theta < 15^\circ$). Figure 8, left shows the mean value of time residuals with respect to a planar fit for different pad multiplicities. The arrival time delay from planar fit increases with distance up to 10 ns for particles landing further than 50 m from the core. No significant dependence on pad multiplicity is observed. In fig. 8, right the real data distribution for $200 < N_{pad} < 400$ is compared with a simulation where Sibyll code has been used for the hadronic interactions and Corsika for the shower development in the atmosphere. No discrepancies are visible and this make us more confident about the tools of this analysis (simulation and reconstruction algorithms).

For primaries interacting deeper in the atmosphere (young showers), due to geometrical reasons, the arrival of particles at a given lateral distance is expected to be more delayed compared to primaries that have interacted higher (old showers). Young showers will then exhibit a steeper time profile with respect to a planar fit. A study of the correlation between the measured shower conicity and the atmospheric depth of the shower maximum suggests to adopt the conicity as an estimator of the shower development stage.

Also events with particularly large time spread have been investigated. They can be grouped into two main typologies: wide shower and double front events. The first ones can be large showers with the core very far from the detector. The second ones are expected to be showers in the same trigger time window ($2\,\mu$s). Some discrepancy with respect to these interpretations could be the signal of exotic effects.

7. – Conclusions

The ARGO-YBJ detector is taking data since November 2007 in the complete setup (central carpet and guard ring) in a very stable way. The detector performances are what expected and they are monitored by the analysis of the Moon shadow in the CR flux. Remarkable results have been achieved in gamma-astronomy [15]. Here a selection of CR physics measurements essentially based on the digital read-out has been presented.

We would like to stress that the analog charge read-out allows to enlarge the energy range of ARGO-YBJ measurements (for istance the p-p cross section measurement) up to thousands of TeV.

* * *

This work is supported in China by NSFC (Contract No. 10120130794), the Chinese Ministry of Science and Technology, the Chinese Academy of Sciences, the Key Laboratory of Particle Astrophysics, CAS, and in Italy by the Istituto Nazionale di Fisica Nucleare (INFN) and the Ministero dell'Istruzione, dell'Università e della Ricerca (MIUR).

REFERENCES

[1] Bacci C. *et al.* (ARGO-YBJ Collaboration), *Nucl. Instrum. Methods A*, **508** (2003) 110; Aielli G. *et al.* (ARGO-YBJ Collaboration), *Nucl. Instrum. Methods A*, **562** (2006) 92.
[2] Aielli G. *et al.* (ARGO-YBJ Collaboration), *Nucl. Instrum. Methods A*, **608** (2009) 246.
[3] He H. H. *et al.*, *Astropart. Phys.*, **27** (2007) 528; Aielli G. *et al.* (ARGO-YBJ Collaboration), *Astropart. Phys.*, **30** (2009) 287.
[4] Aielli G. *et al.* (ARGO-YBJ Collaboration), *Nucl. Instrum. Methods A*, (2011) to be published.
[5] Aielli G. *et al.* (ARGO-YBJ Collaboration), *Astropart. Phys.*, **30** (2008) 85.
[6] Aielli G. *et al.* (ARGO-YBJ Collaboration), *Astroph. J.*, **729** (2011) 113.
[7] Di Sciascio G. and Iuppa R., *Nucl. Instrum. Methods A*, **630** (2011) 301.
[8] Di Sciascio G. *et al.* (ARGO-YBJ Collaboration), *Nucl. Phys. B (Proc. Suppl.)*, **212-213** (2011) 301.
[9] Donato F. *et al.*, *Phys. Rev. Lett.*, **102** (2009) 071301.
[10] Stephen S. A. and Golden R. L., *Space Sci. Rev.*, **46** (1987) 31.
[11] Cirelli M. *et al.*, *Nucl. Phys. B*, **813** (2009) 14.
[12] Blasi P. and Serpico P. D., *Phys. Rev. Lett.*, **103** (2009) 081103.
[13] Aielli G. *et al.* (ARGO-YBJ Collaboration), *Phys. Rev. D*, **80** (2009) 092004.
[14] Gaisser T. K., *Phys. Rev. D*, **36** (1987) 1350; Block M. M., *Phys. Rev. D*, **76** (2007) 111503 and references therein.
[15] Aielli G. *et al.* (ARGO-YBJ Collaboration), *Astrophys. J.*, **699** (2009) 1281; *Astropart. Phys.*, **32** (2009) 47; *Astrophys. J. Lett.*, **714** (2010) L208; Bernardini P. (ARGO-YBJ Collaboration), *Proceedings of Science: Texas 2010* (2010) 166; Bartoli B. *et al.* (ARGO-YBJ Collaboration), *Astrophys. J.*, **734** (2011) 110.